Chromatin Conformation and Salt-induced Compaction: Three-dimensional Structural Information from Cryoelectron Microscopy

Jan Bednar,* Rachel A. Horowitz,‡ Jacques Dubochet,* and Christopher L. Woodcock‡

*Département d'Analyse Ultrastructurale, Université de Lausanne, CH-1015 Lausanne, Switzerland; and‡Department of Biology, University of Massachusetts, Amherst, Massachusetts 01003

Abstract. Cryoelectron microscopy has been used to examine the three-dimensional (3-D) conformation of small oligonucleosomes from chicken erythrocyte nuclei after vitrification in solutions of differing ionic strength. From tilt pairs of micrographs, the 3-D location and orientation of the nucleosomal disks, and the paths of segments of exposed linker can be obtained. In "low-salt" conditions (5 mM NaCl, 1 mM EDTA, pH 7.5), the average trinucleosome assumes the shape of an equilateral triangle, with nucleosomes at the vertices, and a length of exposed linker DNA between consecutive nucleosomes equivalent to ~46 bp. The two linker DNA segments converge at the central nucleosome. Removal of histones H1 and H5 results in a much more variable trinucleosome morphology, and the two linker DNA segments usually join the central nucleosome at different locations. Trinucleosomes vitrified in 20 mM NaCl, 1 mM EDTA, (the salt concentration producing the maximal increase in sedimentation), reveal that compaction occurs by a reduction in the included angle made by the linker DNA segments at the central nucleosome, and does not involve a reduction in the distance between consecutive nucleosomes. Frequently, there is also a change in morphology at the linker entry-exit site.

At 40 mM NaCl, there is no further change in trinucleosome morphology, but polynucleosomes are appreciably more compact. Nevertheless, the 3-D zig-zag conformation observed in polynucleosomes at low salt is retained at 40 mM NaCl, and individual nucleosome disks remain separated from each other. There is no evidence for the formation of solenoidal arrangements within polynucleosomes.

Comparison of the solution conformation of individual oligonucleosomes with data from physical measurements on bulk chromatin samples suggests that the latter should be reinterpreted. The new data support the concept of an irregular zig-zag chromatin conformation in solution over a range of ionic strengths, in agreement with other in situ (McDowall, A. W., J. M. Smith, and J. Dubochet. 1986. *EMBO (Eur. Mol. Biol. Organ.) J.* 5: 1395–1402; Horowitz, R. A., D. A. Agard, J. W. Sedat, and C. L. Woodcock. 1994. *J. Cell Biol.* 125:1–10), and in vitro conclusions (van Holde, K., and J. Zlatanova. 1995. *J. Biol. Chem.* 270:8373–8376). Cryoelectron microscopy also provides a way to determine the 3-D conformation of naturally occurring chromatins in which precise nucleosome positioning plays a role in transcriptional regulation.

THE basic unit of chromatin, the nucleosome core particle, consisting of 145 bp DNA wrapped around an octamer of histones, has been well-characterized. Crystals of the histone octamer have provided high resolution information about all but the free NH_2-terminal domains (Arents et al., 1991), and the core particle has been solved to a resolution of 0.7 nm (Richmond et al., 1984). The chromatosome (Simpson, 1978), comprising two complete turns (166 bp) of DNA and one molecule of the H1 class of very lysine rich (VLR)[1] histones is a more complex particle in which the trajectory of the additional DNA and its relation to the H1 molecule have not yet been fully defined. Chromatin, in which chromatosomes are interconnected by linker DNA, presents an additional level of complexity, and its three-dimensional (3-D) conformation is still less well-understood. It is now well-established that chromatin is not merely a passive mechanism for packing

Address all correspondence to Dr. C. L. Woodcock, Department of Biology, University of Massachusetts, Amherst, MA 01003. Tel.: (413) 545-2825. Fax: (413) 545-1696.

1. *Abbreviations used in this paper*: CTF, contrast transfer function; Dt, diffusion coefficient; GA, glutaraldehyde; VLR, very lysine rich.

© The Rockefeller University Press, 0021-9525/95/12/1365/12 $2.00

DNA, but is the native substrate for transcription, and also plays a key role in transcriptional regulation (e.g., Felsenfeld, 1992; van Holde, 1993; Wolffe, 1994). In some cases, it is changes in chromatin 3-D conformation brought about by precisely located nucleosomes that appear to direct regulatory switches, and it thus becomes important to determine the local spatial relationships of chromatin components.

Much of the current information on chromatin conformation has been obtained from polynucleosomes released from isolated nuclei after micrococcal nuclease digestion. (We use the term polynucleosome rather than isolated chromatin in recognition of the likelihood that isolated material may not reflect the true complexity of the in vivo state [Giannasca et al., 1993].) One aspect of polynucleosome behavior that has a direct bearing on the conformation issue and is open to experimental manipulation is salt-induced compaction. From studies based on a variety of biophysical techniques including sedimentation, light and x-ray scattering, and linear dichroism, as well as direct observation in the electron microscope, it is generally accepted that in low ionic strength solutions (1–5 mM monovalent ions), polynucleosomes assume an open zig-zag conformation in which the linker DNA is extended between consecutive nucleosomes (van Holde, 1988; Butler, 1988; Widom, 1989). Compaction into higher order structures can be reversibly induced by raising the ionic strength of the medium. The relationships between compaction state, ion concentration, and ion valency have been studied in considerable detail, and a mechanism based on electrostatic interactions has been put forward (Widom, 1986; Clark and Kimura, 1990).

Thorough analyses of the sedimentation velocity (S) of different sizes of oligonucleosome over a wide range of salt concentrations have contributed much of the information on the mode of salt-induced compaction in the presence of VLR histones (Butler and Thomas, 1980; Bates et al., 1981). Mono- and dinucleosomes have a constant S value over the 1–100 mM monovalent ion range, while for N = 2 to ~5, an increase in S up to 25 mM NaCl is observed, after which S remains constant. For N> approximately 6, S increases over the whole salt range, a finding interpreted in terms of a requirement for six or more nucleosomes to form and stabilize one turn of a higher order helical chromatin fiber (Butler and Thomas, 1980). Other methods of studying compaction have generally agreed with the sedimentation data, although recent dynamic light scattering measurements of translational diffusion coefficient (Dt) have suggested that dinucleosomes compact in an H1-independent manner in response to increasing salt (Yao et al., 1990, 1991).

In principle, direct observation with the electron microscope should provide definitive information concerning polynucleosome conformation. However, for conventional EM studies, polynucleosomes must be adsorbed to a flat substrate, and then stained or shadowed. In the resulting two-dimensional images, nucleosomes are seen almost exclusively en face, and the 3-D conformation is necessarily lost. Key information concerning the trajectory of linker DNA as it enters and leaves the nucleosome, the flexibility of linker DNA, and the relative orientation of consecutive nucleosomes cannot be obtained. As salt-induced compaction proceeds, it becomes impossible to resolve linker DNA segments with conventional electron microscopy (e.g., Thoma et al., 1979; Woodcock et al., 1984).

The ability to image biological materials freely suspended in vitreous water (Dubochet et al., 1988, 1992) is particularly advantageous for the study of chromatin fragments in solution. An aqueous environment is retained, and, for structures of the size scale of small oligonucleosomes, the complete 3-D conformation may be preserved. From tilt pairs of micrographs, stereology (Beorchia et al., 1991; Dustin et al., 1991), provides 3-D information concerning distances between consecutive nucleosomes, linker DNA trajectories, and the relative orientation of consecutive nucleosomes. We show here that cryoelectron microscopy provides greatly improved images of oligonucleosomes in solution, allowing the results of solution studies on salt-induced compaction to be correlated directly with changes in conformation. Although the qualitative agreement between sedimentation velocity determinations and cryoelectron microscopy is excellent, the conformational changes seen in the microscope show that a reinterpretation of the structural implications of the sedimentation data is necessary.

Materials and Methods

Chromatin Preparation

Fresh chicken blood was diluted into ice-cold 150 mM NaCl, 5 mM Pipes, pH 7.5, 0.5 mM PMSF, and washed twice in the same solution by centrifugation at 1,000 *g*. NP-40 detergent was added to 0.5%, and nuclei pelleted and again washed twice as before. Digestion with micrococcal nuclease (Sigma Chemical Co., St. Louis, MO) was carried out at 37°C in 5 mM Pipes, pH 7.5, containing 0.2 mM $CaCl_2$. After temperature equilibration, enzyme was added to 1 U/50 μg DNA, and the reaction stopped after 2–4 min (when the chromatin gel dispersed), by adding EDTA to 2 mM, and cooling on ice. The soluble chromatin supernatant containing ~40% of the starting material was layered onto linear 5–35% sucrose gradients containing 5 mM NaCl, 1 mM EDTA, pH 7.5, and centrifuged in a rotor (SW27; Beckman Instruments, Fullerton, CA) at 25,000 rpm for 16 h. Fractions were collected using a pump and monitoring system (Isco Inc., Lincoln, NE). Selected fractions were pooled, concentrated, and dialyzed into the desired buffer using Microcon 100 concentrator units (Amicon Inc., Beverly, MA) according to the manufacturer's directions. Concentration occurs by centrifugation of the solution through a porous membrane with a 100,000-D cut-off size.

For removal of histones H1 and H5, samples were brought gradually to 0.6 M NaCl, and Microcon 100 units used first to remove the released histones, and then to restore the NaCl concentration gradually to 5 mM.

Histone content was determined by dissolving chromatin fractions in sample buffer containing SDS and urea, and separating components on 20% polyacrylamide gels containing SDS (Horowitz et al., 1990). In some cases, Coomassie blue–stained gels were digitized using a TV camera (see below), and the summed pixel values corresponding to entire histone bands determined. A series of lanes containing different loadings of histones extracted from whole nuclei was included in each gel, and used for checking the linearity of the analysis procedure.

Dynamic Light Scattering

Chromatin samples were concentrated to 100 μg/ml to 250 μg/ml in three different buffer solutions: 1.0 mM Tris, pH 7.5, 0.01 mM EDTA (Yao et al., 1990); 1 mM Pipes, pH 7.5, 0.1 mM EDTA; and 1.0 mM ETDA, pH 7.5, containing the desired NaCl concentration. After centrifugation at 10,000 *g* for 5 min to remove large particles, light scattering was observed at 20°C in an ALV500 goniometer (ALV-laser, Langen/Hessen, Germany), and translational Dt values calculated using the CONTIN program (Provencher, 1982). At least five 2-min runs were recorded for each sample. Some samples were first fixed with 0.1% glutaraldehyde in the appropriate buffer for 24–48 h, and others were fixed after an initial Dt measurement.

Cryoelectron Microscopy

Chromatin samples were adjusted to ~50 μg/ml in the appropriate NaCl concentration, applied to holey carbon films, and plunged into liquid ethane held just above its freezing point in liquid nitrogen. Some samples were fixed in 0.1% glutaraldehyde at 4°C for 24 h before freezing, then dialyzed into 5 mM NaCl, 1 mM EDTA, pH 7.5. In view of the importance of controlling the evaporation of water from thin films during cryoelectron microscopy (Bellare et al., 1988; Cyrclaff et al., 1990; Bednar et al., 1994), the relative humidity in the specimen area was monitored continuously. No humidity-related changes in chromatin conformation were observed between 60 and 100% relative humidity. Grids were transferred under liquid nitrogen to a cryoholder (model 626; Gatan Inc., Pleasanton, CA), and observed at −170°C in an electron microscope (CM12 or CM10; Philips Electronic Instruments Co., Mahwah, NJ) at nominal magnifications of 42,000 or 45,000. Tilt pairs of micrographs (angular separation 30°) at 1.5–2.0 μm defocus, were recorded in low dose mode, on film (SO-163; Eastman Kodak Co., Rochester, NY), and developed in full-strength D-19 (Eastman Kodak Co.) for 12 min.

Conventional Electron Microscopy

To chromatin samples in the desired salt concentration, glutaraldehyde was added to 0.1% for 24 h at 4°C. Samples were then brought to 50 mM NaCl, and applied to glow-discharged carbon films (Woodcock et al., 1981). Two staining methods were used: in the first, grids were washed with water, then placed on three successive drops of 2% aqueous uranyl acetate, followed by three drops of distilled water, and air dried. In the second, grids were rinsed for 30 s in pH 9 water (50 ml distilled water containing 50 μl of 0.05 M potassium carbonate, potassium borate buffer, pH 10.0) (Fisher Scientific Co., Fairlawn, NJ), containing 0.4% Photoflo 200 (Eastman Kodak Co.), air dried, stained in 1% phosphotungstic acid in 75% ethanol, rinsed in 75% ethanol, 100% ethanol, and air dried. Grids were examined in a Philips CM10 operated at 80 kV, and micrographs taken at a nominal magnification of 39,000.

Image Analysis

Selected micrographs were digitized using either a linear CCD camera (Eikonix 1412; Eastman Kodak, Rochester, NY) (Bednar et al., 1994), or a TV camera (C2400; Hamamatsu Corp., Bridgewater, NJ). The final pixel size was ~0.7 nm^2. Before stereological analysis, image pairs were processed by applying a contrast transfer function (CTF) correction based on the known microscope parameters, and an assumed phase:amplitude contrast ratio of 1:0.07 (Wade and Chretien, 1993). Information at frequencies beyond the first zero of the CTF was suppressed in the final image (Vigers et al., 1986), limiting resolution to 3.1 nm. It was possible to further improve the quality of images with extremely noisy backgrounds by low-pass filtering to 4.7–5.4 nm.

Stereology (Beorchia et al., 1991; Dustin et al., 1991; Furrer et al., 1995) was used to determine 3-D locations of features in the tilt pairs from which coordinates of nucleosome positions and internucleosomal distances and angles were derived. Where possible, x,y,z coordinates were determined for nucleosome centers and linker DNA entry-exit sites, and several points along each linker DNA and used to calculate the following parameters (see Fig. 2): cc, center-to-center distance between consecutive nucleosomes; ee, distance between linker entry-exit sites; L, length of spline fit to points along linker DNA; a, included angle at the point of divergence of two linker DNA segments; and b, included angle at the center nucleosome determined from nucleosome centers. The reproducibility of these measurements was tested as follows: the mean of the standard deviation in point selection (five trials) in the 2-D images was 0.6 pixels. The effect of point-picking error on 3-D calculations was estimated by allowing 2-D coordinate values to vary by 1–3 pixels. A two pixel change in a 2-D coordinate resulted in a 3-D distance change of less than one pixel, and a 3-D angle change of less than one degree. To assess operator bias in point selection, a data set of 33 trinucleosomes was analyzed by two operators at different sites, each using independently developed software. Each trinucleosome was analyzed five times by each operator. There were no significant differences between the calculated 3-D distances (t test, $P = 0.87$), or 3-D angles (t test, $P = 0.99$).

The orientations of nucleosome disks were determined from peak correlation coefficient values (>0.85) after cross-correlation with a set of 360/5° projections of a model nucleosomal disk. This disk was modeled to the dimensions determined by x-ray crystallography (Richmond et al., 1984). The inner radii, representing protein, and the outer radii, representing DNA, were assigned densities at a ratio of 0.6:1.0, based on mean pixel intensities measured on frozen-hydrated images of en face nucleosomes. Individual nucleosomes from the first image of a frozen-hydrated image pair were oriented in the 2-D image plane to a common axis, defined by the site at which linker DNA joined the nucleosome, before the cross-correlation. Since the model nucleosome disk is symmetrical, two correlation peaks separated by 180° are found. The symmetry of the disk also results in identical peaks for projections of equal positive and negative rotation relative to the 0° projection. Final assignment of nucleosome orientation depended on the combination of the rotation data with the stereological data set, consisting of 3-D coordinates, internucleosomal distances, and dimensions. Solid models of selected oligomers were created by positioning objects of appropriate dimension representing nucleosomal disks and linker DNA paths at the coordinates and orientations derived as described above. These models were examined interactively in three dimensions using Vertigo 9.6 (Vertigo, Inc., Vancouver, B.C., Canada) software. Comparison of stereo-pair projections of the resulting solid model with the original stereo-pair images provides an additional means of evaluation and refinement of the models. Image processing and analysis were performed on a Silicon Graphics workstation using the SUPRIM (Bretaudiere, J. P., and J. Schroeter, University of Texas; revisions by B. Carragher, Beckman Institute, University of Illinois) image processing package.

Results

We have used cryoelectron microscopy to determine the 3-D solution conformation of chicken erythrocyte oligonucleosomes. This chromatin has a mean nucleosomal repeat of ~212 bp, and three VLR histones, H1A, H1B, and H5 (van Holde, 1988), with H5 estimated to be present at a ratio of 0.9 molecules per nucleosome, and the two H1 variants to total 0.4 molecules per nucleosome (Bates and Thomas, 1981). The sedimentation behavior of chicken erythrocyte oligonucleosomes has been studied in detail, and shown to be qualitatively similar to that of rat liver (Bates et al., 1981).

Oligonucleosomes were prepared from isolated chicken erythrocyte nuclei by digestion with micrococcal nuclease, and separation on sucrose gradients. A low salt environment (<5 mM monovalent ions) was maintained during digestion and subsequent handling to avoid redistribution of the VLR histones H1 and H5 (Caron and Thomas, 1981; Thomas and Rees, 1983). Peak fractions corresponding to oligonucleosomes with N = 1,2,3,4, and N = 5–15 were collected and dialyzed into 5 mM NaCl, 1.0 mM EDTA, pH 7.5. The histone content of the trinucleosome fraction relative to the starting nuclei was estimated from the total Coomassie blue stain intensity of individual bands on SDS gels. Over a range of sample loadings of total protein from whole nuclei, the ratio of stain intensity in the histone H4 band to intensity in the histone H5 band had a constant value of 2.4, while trinucleosome preparations gave a ratio of 2.9. This indicates that, compared with whole nuclei, the trinucleosomes were depleted in H5 by ~17%. This is similar to the 15% reduction of VLR histones in dinucleosome fractions reported by Yao et al. (1990), and is probably due to their partial loss from the two end nucleosomes.

Imaging of Frozen Hydrated Oligonucleosomes

Samples were applied to holey carbon films, cryoimmobilized by plunging into liquid ethane, and micrographs recorded at −170°C (Bednar et al., 1994). A tilt pair of micrographs was recorded for each specimen area to retrieve

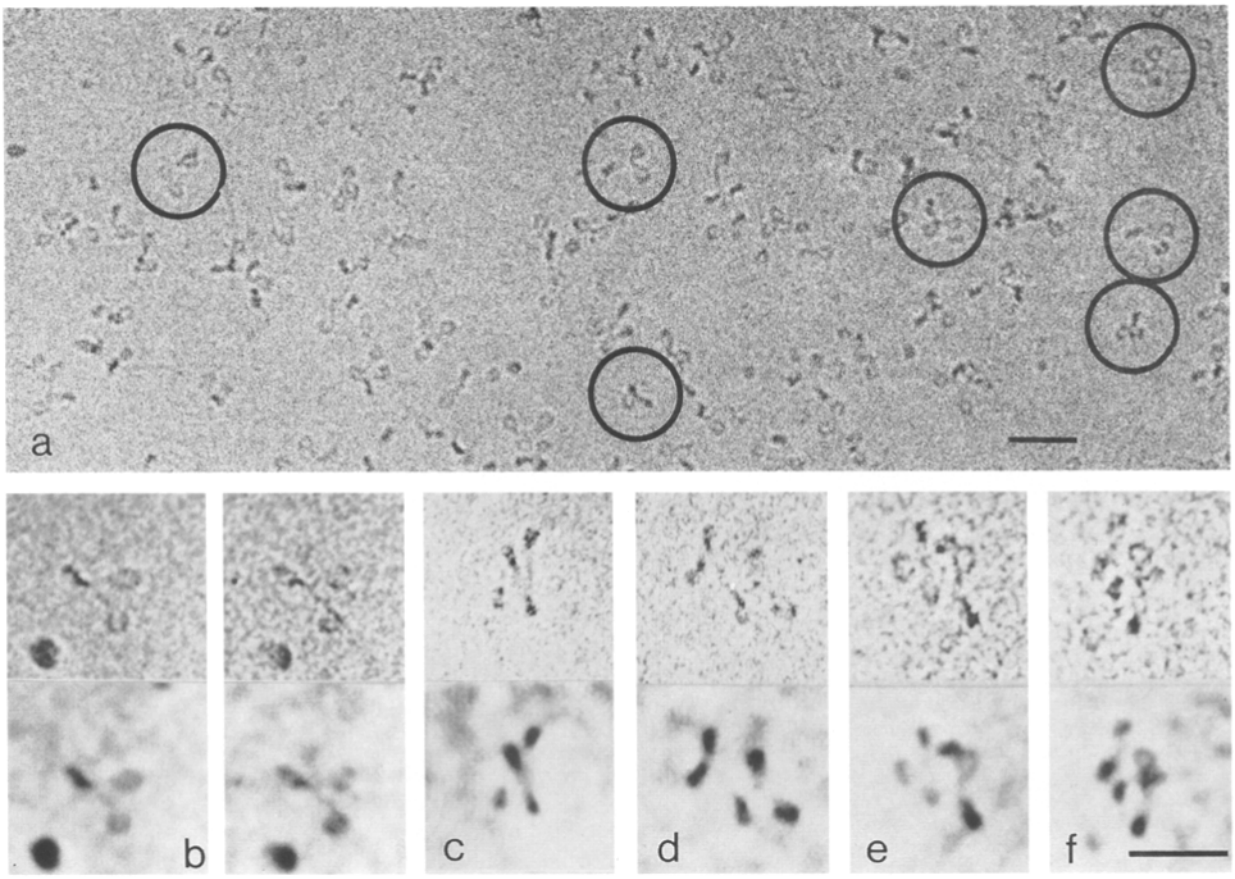

Figure 1. (*a*) Survey view of a trinucleosome fraction vitrified in a thin film of 5 mM NaCl. Some clearly defined trimers have been circled. (*b–f*) Selected examples of images of frozen hydrated oligonucleosomes vitrified in 5 mM NaCl, illustrating the zig-zag structures formed by nucleosomes and linker DNA. Raw images are shown in the upper row, CTF corrected images in the lower row. (*b*) The two tilt images of a trinucleosome. (*c–f*) Tetra-, penta-, and hexa-nucleosome images. Bars, 50 nm.

3-D information (Dustin et al., 1991). To obtain useful images of the inherently low contrast, unstained vitrified oligonucleosomes, a nominal underfocus of 1.5–2.0 μm was used (Dubochet et al., 1988), resulting in images such as those shown in Fig. 1, *a* and *b–f*. The determination of 3-D coordinates via stereology requires the identification of matched points of features in each image of the tilt pair. To avoid erroneous identification of features based on artefactual edges generated by the strong defocus, a CTF correction was applied (see Materials and Methods). Suppression of information beyond the first zero of the CTF resulted in a limiting resolution of 3.1 nm. The processed images (Fig. 1, *bottom row*), with a more accurately defined nucleosome envelope and lower background, were used for all image-based analyses. Unless noted, only single images from the stereo pairs used for analysis are shown in the figures.

The best image pairs yield the location and orientation of each nucleosome and the path of linker DNA segments between them, from which a 3-D model such as that shown in Fig. 2 can be built. In cases where a complete linker path (*L*, Fig. 2) cannot be determined, useful information may be obtained from the 3-D center-to-center distance between consecutive nucleosomes (*cc*, Fig. 2) and/or the distance between linker entry-exit points (*ee*, Fig. 2).

Chromatin Conformation in 5 mM NaCl

Trinucleosomes are the simplest polymer containing a complete chromatosome. We have therefore examined frozen

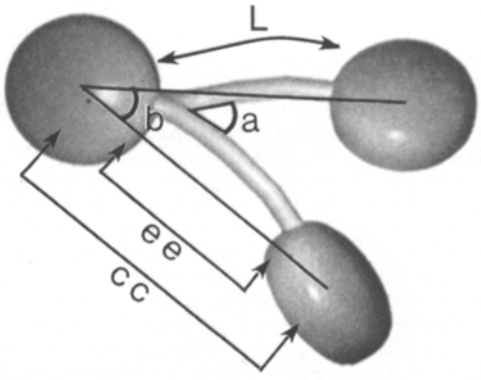

Figure 2. Trinucleosome model illustrating the measured parameters. *L*, actual 3-D length of exposed linker. *ee*, 3-D distance between linker ee sites. *cc*, 3-D distance center-to-center distance between consecutive nucleosomes. *a*, 3-D angle between entering and exiting linker segments. *b*, 3-D angle between consecutive nucleosome centers.

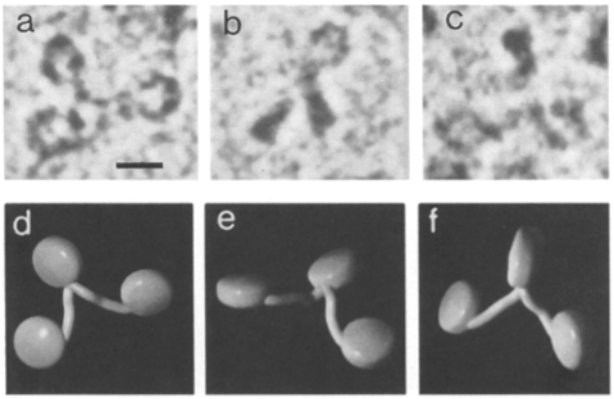

Figure 3. Trinucleosome morphology in 5 mM NaCl. (*a–c*) Three individual particles with nucleosomes in a range of orientations. Bar, 10 nm. (*d–f*) A solid model representation of the trinucleosome shown in *a* viewed from different angles. The model illustrates the single linker ee point at the center nucleosomes, and the extended linker DNA commonly observed at this ionic strength.

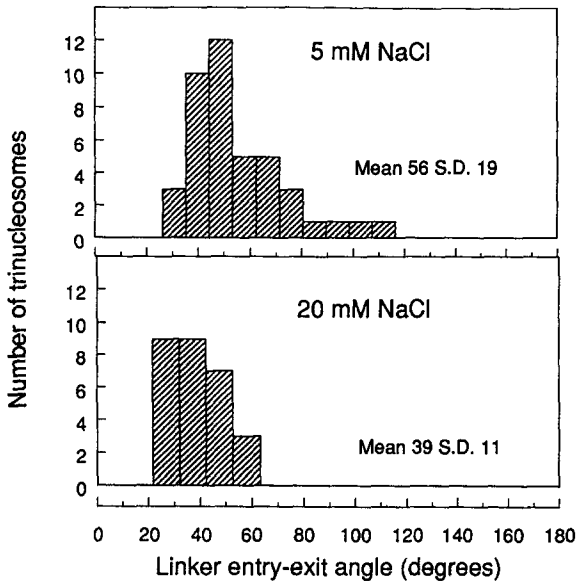

Figure 4. Distribution of 3-D linker ee angles (angle a, Fig. 2) in trinucleosomes vitrified in 5 mM NaCl (*top*) and 20 mM NaCl (*bottom*).

hydrated trinucleosomes in some detail, concentrating on the morphology of the central nucleosome, the angle between the two linker DNA segments, and the length of the linkers. Fig. 1 *b* shows a tilt pair of micrographs obtained from a vitreous thin film of trinucleosomes in 5 mM NaCl, 1 mM EDTA, pH 7.5, and in Fig. 3, higher magnification views of three others are presented, together with model representations of one of them. As expected for freely suspended particles, many different views of trinucleosomes are obtained, and there appears to be no favored orientation nor entrapment at either of the two air interfaces. In contrast to conventional EM where nucleosomes typically appear en face, the nucleosomal disks are seen in a variety of orientations. The disks have a mean diameter of ~11 nm when viewed en face, and a thickness of ~6 nm when viewed on edge, in agreement with x-ray data (Richmond et al., 1984).

In cases where the path of the linker DNA between the three nucleosomes is sufficiently clear to identify which nucleosome occupied the central position, the two linker segments typically converge at a single site on the nucleosomal disk (Fig. 3). The distribution of included angles made by linker DNA segments at the center nucleosome (*a*, Fig. 2) is shown in (Fig. 4 *a*). The mean value of 56° (SD, 19°) indicates that the average low salt trinucleosome conformation resembles an equilateral triangle with nucleosome disks at the vertices.

Distance between Nucleosomes

From the stereo pairs, the 3-D distances L, ee, and cc (Fig. 2) were determined (Table I). L is the length of a spline fit to measured points along the linker and the most accurate estimate of the length of exposed linker. Its mean value of 48 bp (SD, 12 bp) is close to the expected value of 46 bp for chromatin with a 212-bp nucleosome repeat, of which 166 bp is wrapped around the chromatosome (Simpson, 1978). The somewhat shorter 3-D distance between linker entry-exit points (ee) may be due to linker DNA bending; however, the large standard deviations of these length measurements (see below) makes differences of 2 nm statistically insignificant. The center-to-center distance between nucleosomes (*cc*, Fig. 2) provides the least direct estimation of exposed linker length, since its use assumes that nucleosome centers and linker ee points lie on a straight line (see Fig. 2). For trinucleosomes at 5 mM NaCl, the cc−11 value provides a rough approximation of the length of exposed linker.

Lengths of the Two Linkers of a Trinucleosome Are Strongly Correlated

Linker lengths (L) ranged from 7.1 nm (~21 bp) to 23.8 nm (~70 bp), consistent with the ~65-bp span of trimmed dinucleosomes reported by Prunell and Kornberg (1982) for rat liver chromatin. There is a strong correlation ($r^2 = 0.85$) between the lengths of the two linker DNA segments of trinucleosomes (Fig. 5). Since the material was never exposed to conditions that favor octamer sliding (Pennings et al., 1991, 1994), it is unlikely that this result is due to the

Table I. 3-D Lengths Measured from Tilt Pairs of Frozen Hydrated Trinucleosomes Vitrified in 5 and 20 mM NaCl

NaCl concentration	Parameter	Mean 3-D distance	Base pair equivalent	Number of measurements
mM		*nm*		
5	L	16.2 SD 4.1	48	20
5	ee	14.4 SD 4.1	42	28
5	cc	28.5 SD 6.7	–	38
5	cc−11 nm	17.5	51	38
20	L	15.2 SD 1.5	45	10
20	ee	13.6 SD 4.0	40	22
20	cc	25.0 SD 5.7	–	22
20	cc−11 nm	14.0	41	22

The parameters *L*, actual length of exposed linker DNA, *ee*, distance between linker entry-exit sites, and *cc*, center-to-center distance between consecutive nucleosomes represent three different methods of estimating the 3-D length of exposed linker DNA, and are defined graphically in Fig. 2. For the bp equivalent, initial measurements in nm have been converted assuming 1 bp = 0.34 nm.

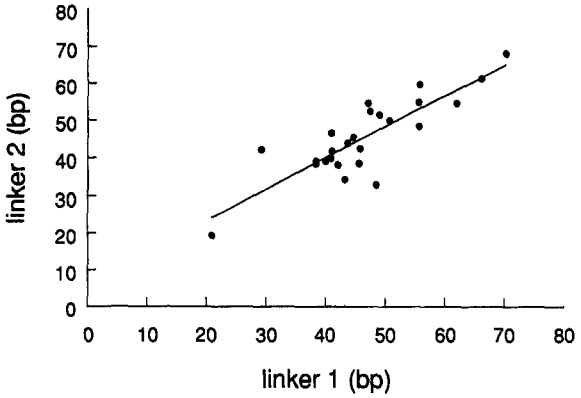

Figure 5. Correlation between the 3-D lengths of the two exposed linker DNA segments (*L*, Fig. 2) of trinucleosomes vitrified at 5 mM NaCl expressed as base pairs (*bp*). Although there is a wide range of linker lengths (~50 bp), they are strongly correlated ($r^2 = 0.85$) in individual trinucleosomes.

postdigestion centering of the middle nucleosome. In the absence of sliding, the observed correlation indicates that consecutive nucleosomes tend to have similar linker lengths, a conclusion also suggested by analysis of mononucleosomal DNA length distributions (Todd and Garrard, 1979).

Removing Histones H1 and H5 Changes Chromatosome Morphology

Trinucleosomes were also examined in the frozen hydrated state after removing most of the VLR histones with 0.6 M NaCl. SDS gel analysis of the remaining proteins confirmed that only a trace of VLR histones was retained after this treatment, and that the core histones were still present in equimolar amounts (not shown). After VLR histone removal, trinucleosomes were much more variable in shape, with a wider range of included angles at the center nucleosome. Often, the two linker DNA segments did not join the center nucleosome at the same site (*arrowheads*, Fig. 6); a more dramatic unwrapping of DNA from the center nucleosome was also seen in some cases (Fig. 6 *f*). These changes in chromatosome morphology are consistent with the role of the VLR histones in stabilizing the two turns of chromatosomal DNA (Allan et al., 1980), with the observed loss of a zig-zag chromatin morphology after VLR histone removal (Thoma and Koller, 1977), and with the H5-dependent morphology of nucleosomes reconstituted onto small DNA circles (Zivanovic et al., 1990).

Another feature common among VLR histone–depleted trinucleosomes, but rarely seen in images of complete trinucleosomes, is the presence of a linker DNA fragment extending from one of the outer nucleosomes (Fig. 6, *arrows*). These fragments have a mean length of 43 bp (SD, 15 bp; N = 14), close to the mean linker length (45 bp; SD, 11; N = 14) between nucleosomes in the same trinucleosomes. It is unlikely that these end fragments resulted from sliding of the outer nucleosome, as this would produce a concomitant reduction in the adjacent internucleosomal distance.

Morphology of Higher Oligonucleosomes

The solution conformation of polynucleosomes at 5 mM

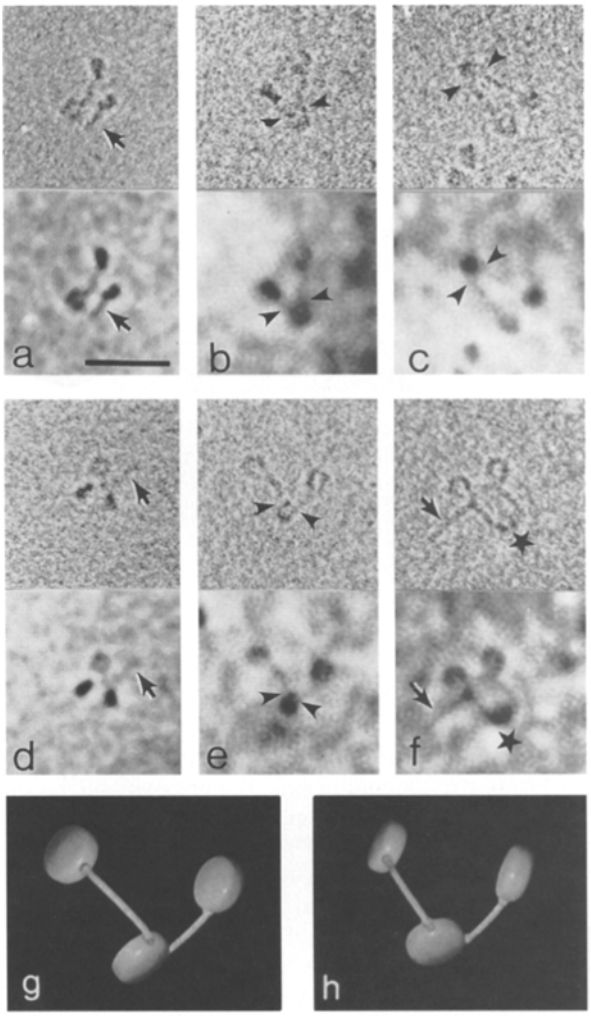

Figure 6. Gallery of trinucleosomes depleted in VLR histones and vitrified in 5 mM NaCl. For *a–f*, the raw images are shown above, and the CTF-corrected images below. In *b*, *c*, and *e*, linker DNA segments join the center nucleosome at separate sites (*arrowheads*), and *a*, *d*, and *f* show linker fragments emanating from one of the outer nucleosomes (*arrows*). More extensive unfolding of nucleosomal DNA is seen in *f* (*asterisk*). Two views of a solid model of the trinucleosome in *e* are shown in *g* and *h*. Bar, 50 nm.

NaCl is a 3-D zig-zag structure, continuing the pattern described for the trinucleosome (Fig. 1, *b–e*). The zig-zag is not a flattened ribbonlike structure as seen by conventional microscopy (e.g., Rattner and Hamkalo, 1978; Thoma et al., 1979), where nucleosomes are all seen en face due to adsorption to the substrate.

Chromatin Conformation in 20 mM NaCl

Both physical measurements on bulk samples and direct imaging show that the change in ionic conditions between 5 and 20 mM monovalent ions results in chromatin compaction. For trinucleosomes, the maximum sedimentation value is obtained at 20 mM NaCl (Butler and Thomas, 1980; Bates and Thomas, 1981).

Representative images of frozen hydrated trinucleosomes equilibrated in 20 mM NaCl, 0.1 mM EDTA, pH 7.0, are shown in Fig. 7, one of which (Fig. 7 *a*) is presented as a solid model viewed from different directions (Fig. 7, *d–f*). While

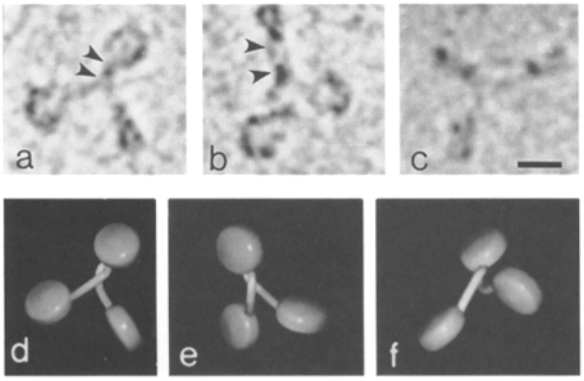

Figure 7. Trinucleosome morphology in 20 mM NaCl. (*a–c*) The two linker segments tend to come together before joining the center nucleosome (*arrowheads*). In some cases (*c*), it is not possible to determine which nucleosome is the center one. Scale is 10 nm. (*d–f*) Views of a solid model representation of the trinucleosome in *a*.

the general morphology of trinucleosomes is similar in 5 and 20 mM NaCl, there is a distinct change at the central nucleosome, where the two linker DNA segments tend to converge 5–10 nm distal to the nucleosomal disk at the higher ionic strength. This change is accompanied by a significantly ($P < 0.05$) smaller included angle of 39° (SD, 9°) at 20 mM NaCl than at 5 mM. Comparison of the angle data (Fig. 4) shows that the 17° change in mean-included angle is due to a reduction in the range of angles at 20 mM NaCl in addition to a small shift in the overall distribution. The minimum included angles are very similar at both ionic strengths. Thus the compaction of trinucleosomes that results in an increased sedimentation velocity (Butler and Thomas, 1980; Bates and Thomas, 1981) and translational diffusion coefficient (see below), occurs by a reduction in the mean angle between the two linker segments, effectively bringing the two outer nucleosomes closer to each other. This mode of compaction is also observed in tetra- and pentanucleosomes (not shown).

Internucleosomal Distance Does Not Change between 5 and 20 mM NaCl

The mean distance between consecutive nucleosomes in a trimer does not change significantly between 5 mM and 20 mM NaCl. As shown in Table I, both the actual lengths of exposed linker, and the 3-D distance between linker ee points are very similar at these ionic strengths. This observation is at variance with a recent series of publications by Yao et al. (1990, 1991, 1993) reporting that dinucleosomes from chicken erythrocytes showed an increase in translational Dt over the 1–20 mM range of monovalent ions. The Dt increase was correlated with a substantial reduction of internucleosomal distance as measured from electron micrographs of stained, glutaraldehyde (GA)-fixed material, and did not require the presence of VLR histones (Yao et al., 1991). The conclusion was that dinucleosomes were subject to salt-induced compaction, and that the compaction process occurred through linker coiling.

The disparity between these results and the trinucleosome data described above prompted an examination of frozen hydrated dinucleosomes. Representative images of

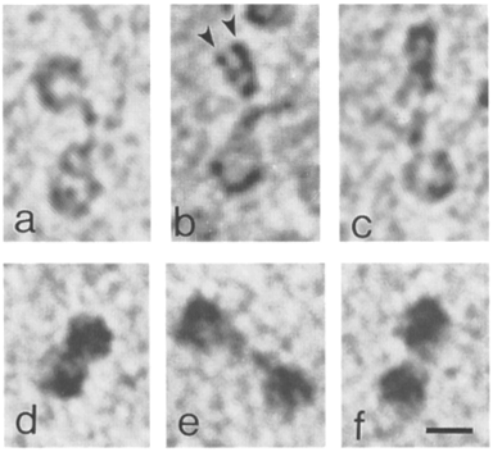

Figure 8. Dinucleosome morphology in 20 mM NaCl. (*a–c*) Frozen hydrated images appear similar to those of trinucleosomes (Fig. 7), and in favorable views, the two turns of DNA are seen (*arrowheads*, *b*). In contrast, conventional EM images of stained preparations (*d–f*) show both nucleosome disks en face, and are less informative structurally. In most cases, the nucleosomes are closer together in conventional EM preparations. Bar, 10 nm.

vitrified dinucleosomes recorded in 20 mM NaCl, 0.1 mM EDTA, pH 7.0, are shown in Fig. 8, *a–c*. In frozen hydrated preparations, the linker clearly remains extended. The mean center-to-center distance between nucleosomes is 30.3 nm (SD, 5.1 nm), indicating a minimum exposed linker length of 57 bp (Fig. 9), considerably longer than the expected value of ~46 bp for this chromatin, and suggesting that the linker must include some DNA unwound from the chromatosome. We also examined di- and trinucleosomes in 20 mM NaCl by conventional EM after adsorption to a carbon substrate and staining (Fig. 8, *d–f*). These had a very different distribution of morphologies from the frozen hydrated preparations. The nucleosomes were usually seen en face, and the mean center-to-center distance was equivalent to an exposed linker 14 bp in length (Fig. 9). In ~25% of the particles, the two nucleo-

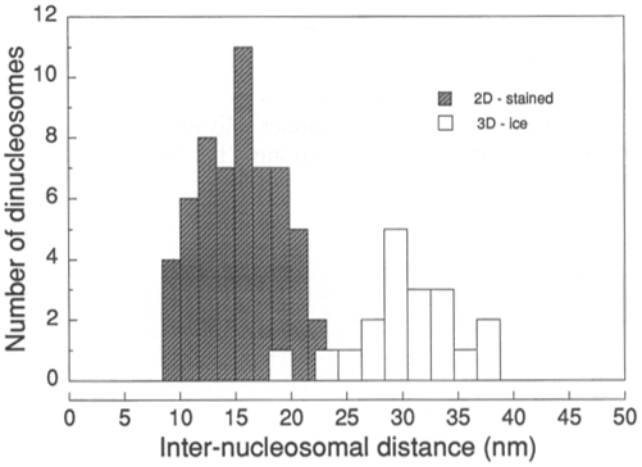

Figure 9. Distribution of internucleosome distances (*cc*, Fig. 2) in frozen hydrated dinucleosomes (*open bars*), and conventionally prepared dinucleosomes (*hatched bars*).

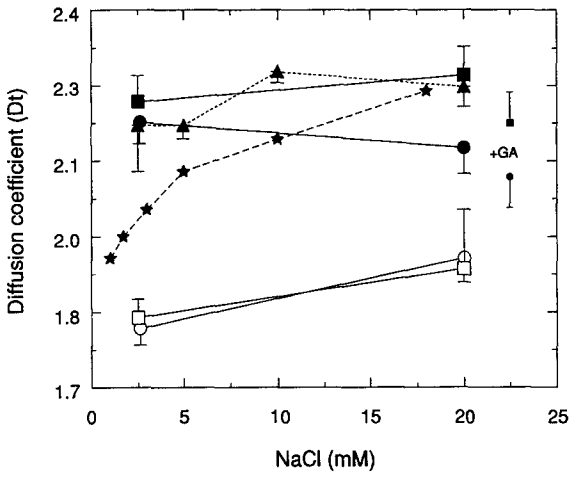

Figure 10. Translational Dts for dinucleosomes (*closed symbols*) and trinucleosomes (*open symbols*) at different salt concentrations and in different buffer solutions (see Materials and Methods for details). Trinucleosomes show a significant salt-induced increase in Dt indicating compaction of these particles. In contrast, no significant change in Dt is observed for dinucleosomes. For two of the dinucleosome preparations, Dt values were remeasured after fixation in 0.1% glutaraldehyde for 24 h (+GA), and found not to change significantly. Error bars show one SD. Also included are data reported by Yao et al. (1991) for dinucleosomes containing VLR histones (*star symbols*). -▲-, Dimer-Tris; —●—, Dimer-EDTA; —■—, Dimer-Pipes; —○—, Trimer-EDTA; —□—, Trimer-Pipes; -★-, from Yao et al., 1991.

some disks were touching (Fig. 8 *d*). Dinucleosome morphology was similar in preparations stained with ethanolic phosphotungstic acid or aqueous uranyl acetate (not shown).

Dynamic light scattering was used to obtain translational Dt values of dinucleosomes for a range of ionic strengths, and in three different buffer solutions including the Tris buffer used by Yao et al. (1990, 1991). Dinucleosome fractions were dialyzed into the desired buffer, centrifuged to remove any large particulate matter, and light scattering data collected (Fig. 10). While the initial Dt values of 2.2 $cm^2/s \times 10^7$ are similar to those reported by Yao et al. (1990) for dinucleosomes in 2.5-mM monovalent ions, there is no significant change in Dt between 2.5 and 20 mM NaCl for any of the three solvents. Trinucleosomes do, however, show a significant Dt increase between 5 and 20 mM NaCl (Fig. 10).

To determine whether aldehyde fixation produced a change in the compaction state, GA was added to some samples in 20 mM NaCl immediately after Dt determination, and a second set of readings taken after 24 h at 4°C. Fixation of dinucleosomes produced only a small change in mean Dt value (Fig. 10), unlikely to account for the difference in morphology we observed between frozen hydrated and fixed and stained dinucleosomes. Based on the present evidence, it seems most likely that dinucleosomes incur an altered conformation during the processes of adhesion to the support film, and/or air drying, accounting for the differences between our data from frozen hydrated images and those of Yao et al. (1990, 1991) using conventional EM. The differences between our Dt measurements and those of Yao et al. (1990) are unlikely to be due to a loss of VLR histones, as Yao et al. (1991) reported identical Dt changes in dinucleosomes stripped of VLR histones.

Chromatin Conformation above 20 mM NaCl

Sedimentation studies suggest that an additional mode of compaction occurs in hexanucleosomes and higher oligomers above 20 mM NaCl (Butler, 1988). Whereas the smaller oligomers (3–5 nucleosomes) show no increase in sedimentation velocity (S) above ~20 mM NaCl, the S value of larger chromatin particles continues to increase. To determine the morphological basis of this change, we examined oligonucleosomes in the frozen hydrated state at 5 and 40 mM NaCl.

Cryoelectron microscopy at ionic strengths above ~20 mM monovalent ions is complicated by the tendency of nucleosomes to dissociate, a phenomenon that is not understood, but appears to be related to the attraction of chromatin to the air solvent interface where surface denaturation may occur. It is most unlikely that the observed dissociation is caused by an artifactual elevation of salt to the ~1.0 M concentration required for histone–DNA dissociation in solution. Although evaporation of water from thin films is a concern in cryoelectron microscopy (Dubochet et al., 1988), studies examining the phenomenon in detail suggest that under the controlled humidity conditions used here, the effect is minimal (Bellare et al., 1988; Cyrklaff et al., 1990). The artifact can be prevented by prefixing with GA (as is necessary for conventional EM of chromatin), but the fixation process itself could produce changes in conformation. To address this issue, trinucleosomes were prefixed in 5 and 20 mM NaCl, vitrified, examined in the frozen hydrated state, and the images analyzed as described above. We were unable to detect any significant qualitative or quantitative differences between the fixed and unfixed material at these ionic strengths (not shown), suggesting that, within the resolution limits of our methodology, prefixation does not cause measurable changes in oligonucleosome morphology.

Polynucleosomes were adjusted to 5 or 40 mM NaCl, fixed with glutaraldehyde as described, and vitrified preparations made. In agreement with sedimentation data, trinucleosomes have the same triangular conformation at 40 mM NaCl as at lower ionic strengths (Fig. 11 *a*), whereas with larger polynucleosomes a response to increased salt is observed. At 5 mM NaCl, larger polynucleosomes appear in a 3-D zig-zag conformation (Fig. 1, *c–f*), and the included angle between three consecutive nucleosomes is the same as that observed in trinucleosomes at that ionic strength (data not shown). Polynucleosome conformation in 40 mM NaCl is illustrated in Fig. 11, *b–d*. Individual nucleosomes are usually well-resolved in the frozen hydrated preparations, although the additional compaction results in superposition and overlap of structures in the z direction that limits the analysis of many images. In contrast, in conventional EM preparations, polynucleosomes in 40 mM NaCl generally appear as an unresolved aggregate of nucleosomes (e.g., Thoma et al., 1979; Woodcock et al., 1984). From a large population of polynucleosome images, cases where three or more consecutive nucleosomes could be identified were selected, and the internucleosomal an-

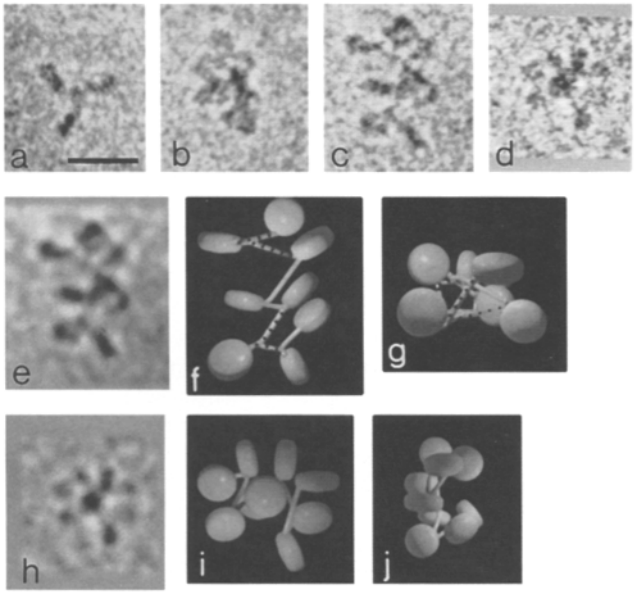

Figure 11. Morphology of oligonucleosomes in 40 mM NaCl. Although trinucleosomes (*a*) appear similar to those observed at lower salt concentrations, polynucleosomes (*b–d*) appear more compact than at lower ionic strengths. Bar, 30 nm. *e* is the CTF-corrected image of the polynucleosome shown in *c*, and *f* and *g* two views of its solid model representation. The polynucleosome in *d* has been similarly analyzed in *h–j*. Modeling reveals that a 3-D zig-zag conformation is retained at 40 mM NaCl, with individual nucleosomes separated from each other in 3-D space. Comparison of *f* with *g* and *i* with *j* shows that the degree of compaction cannot be estimated from a single view.

gles measured. The mean value of 46° (SD, 11°; N = 28) is not significantly different from that of maximally compacted trinucleosomes at 20 mM (Fig. 4), but there is a decrease in the center-to-center distance between nucleosomes (mean 16.9 nm; SD, 4.2 nm; N = 67). In the subset of these images where linker paths could be analyzed (N = 9), the mean linker length (L) is 15.8 nm, SD, 7.9 nm; corresponding to ~46 bp DNA, and very similar to the length of exposed linker at lower ionic strengths (Table I). For these linker segments, the distance between ee is 13.2 nm, SD 4.3 nm, the straight line (ee) distance being ~16% shorter than the actual linker path length. These linkers were extended between nucleosomes in a gently curved path.

Model representations of two 40 mM NaCl polynucleosomes are shown in Fig. 11, *f*, *g*, *i*, and *j*. The 3-D positions and orientations of each nucleosome were first determined, as well as any clear linker paths, and linker ee sites. Putative linker DNA connections were then estimated, based on ee sites and allowable linker lengths. Putative linker DNA is shown as straight connections between nucleosomes, while observed linkers follow the actual path and are stippled. Examination of the models from different views (Fig. 11, *f*, *g*, *i*, and *j*) makes it clear that single projections can give very misleading impressions both of polynucleosome architecture and extent of compaction. The compact appearance of the polynucleosome shown in Fig. 11 *b* in which nucleosomes seem to touch one another is likely to be due to this effect. The models confirmed that at 40 mM NaCl, individual nucleosomes did not touch their closest neighbors. Further, there were no indications of face-to-face aggregations of nucleosomes, nor the incipient formation of solenoidal or other regular packing arrangements.

Discussion

Frozen Hydrated Imaging of Chromatin

Imaging in vitreous water has proven very advantageous for biological structure determination, and has been used successfully on a wide range of specimens (Adrain et al., 1984; Stewart and Vigers, 1986; Dubochet et al., 1988, 1992; Wade and Chretien, 1993). The technique allows the material to be observed in an aqueous environment, and also prevents delicate material being flattened by adhesion to a support film and subsequent dehydration. Unfixed samples can be vitrified successfully at 5, 10, and 20 mM NaCl, and the surface interactions that appear to distort nucleosome morphology at higher ionic strengths can be prevented by mild fixation. Comparison of fixed and unfixed chromatin fragments at 20 and 5 mM NaCl suggests that any fixation-induced changes are below the resolution of our frozen hydrated images. A similar conclusion was reached from studies of frozen hydrated sections of nuclei (Woodcock, 1994), and a detailed x-ray study of isolated chromatin fibers also found that fixation produced minor changes in scattering within the fibers (Williams and Langmore, 1991).

Images of frozen hydrated polynucleosomes are much more informative than those produced by conventional EM. In addition to the preservation of the 3-D solution conformation, the absence of heavy metal staining produces inherently higher resolution (compare Fig. 8, *a–c* and *d–f*). This allows the trajectory of both nucleosomal and linker DNA to be mapped with greater precision than heretofore. Less information is provided about the histone core, which is contrasted much more weakly than DNA.

The Solution Conformation of Chromatin Is an Irregular 3-D Zig-Zag

In the presence of VLR histones, nucleosome-linker DNA units adopt a 3-D zig-zag structure, the key elements of which are chromatosome architecture and extended linker DNA. Cryoelectron microscopy provides the clearest images to date of the path of linker DNA as it enters and exits the nucleosome (Figs. 1 and 3). At low salt (5 mM NaCl), the entering and exiting linker DNA segments join the nucleosome disk at the same location (Figs. 1 and 3), with a mean included angle of 56° (Fig. 4). In no instances have we observed a linear beads on a string conformation or a stacked face-to-face arrangement of nucleosomes. The present data on material that is neither fixed nor attached to a flat substrate confirms that, in solution, chromatin is folded in a 3-D zig-zag conformation.

Salt-induced Compaction

Developing a complete description of salt-induced chromatin compaction in vitro is an important step in understanding the behavior and properties of chromatin in the physiological ionic strengths present in the living nucleus.

At one level, the combination of charge shielding and neutralization provides an effective description of the electrostatic interactions that dictate the compaction state of chromatin (Clark and Kimura, 1990). While this theory does not address the critical details of nucleosome–linker DNA arrangements, the extensive literature on chromatin compaction in solution documents several phenomena with a direct bearing on these issues. Although compaction may occur in the absence of VLR histones (Hansen et al., 1989; Garcia-Ramirez et al., 1992), only in the presence of these histones is the zig-zag morphology observed, and the end product fiberlike (Thoma et al., 1979; Allan et al., 1982). By dictating the structure of the chromatosome, the VLR histones establish a basic chromatin architecture upon which compaction acts. The low salt zig-zag conformation is dependent on the globular and COOH-terminal domains of the VLR histones (Thoma et al., 1983; Losa et al., 1984; Allan et al., 1986), and on the NH_2-terminal domains of the core histones (Allan et al., 1982; Garcia-Ramirez et al., 1992).

Sedimentation and light scattering studies show that the extent of compaction depends on the size of the polynucleosome fraction (Butler and Thomas, 1980; Marion et al., 1981): dinucleosomes do not compact in response to salt, small oligonucleosomes (N = 3 to ~5) compact between 1 and 20 mM monovalent ions, but do not change thereafter, and higher polynucleosomes (N = ~6+) compact over the entire 1–100 mM range. Cryoelectron microscopy makes it possible to define the specific morphological changes that give rise to these physicochemical phenomena.

Chromatosome Conformation Changes in Response to Salt

In the presence of VLR histones, key changes occur near the ee site of the linker DNA (Figs. 3 and 7). The morphology at 20 mM NaCl, where the two linker segments lie parallel to each other for 5–10 nm (Fig. 7) indicates that over this distance, the mutual repulsion of the two linker segments is counteracted. This could occur by a combination of charge shielding by monovalent ions, and charge neutralization by VLR histones, perhaps mediated by the COOH-terminal domains (Allan et al., 1986). As a result, the mean internucleosomal angle is reduced (Fig. 4). For tri- and tetranucleosomes, further increases in ionic strength have no obvious morphological effects (Fig. 11 *a*), in accordance with sedimentation (Butler and Thomas, 1980) and light scattering (Marion et al., 1981) measurements. Higher oligomers do, however, show increased compaction at 40 mM NaCl (Fig. 11, *b–d*).

What differences between trinucleosomes and polynucleosomes account for this change? We can now rule out the explanation that a hexanucleosome allows a complete turn of a helical chromatin fiber to be formed (Butler and Thomas, 1980; Butler, 1988). Frozen hydrated images show no signs of incipient helix formation, nor the face-to-face nucleosomal contacts required for this type of architecture. On the contrary, nucleosomes remain separated from each other in 3-D space in 40 mM NaCl. A similar conclusion was reached from tomographic analyses of chromatin fibers in situ (Horowitz et al., 1994). The absence of close contacts between nucleosomes is also consistent with a number of chemical cross-linking studies showing very little change in histone–histone contacts (Lennard and Thomas, 1985; Hardison et al., 1977) or histone–DNA contacts (Bavykin et al., 1986) between chromatin in its native compact state, and after low salt dispersal. The principal change observed by cryoelectron microscopy at 40 mM NaCl is an ~15% reduction in the distance between consecutive nucleosomes.

The molecular events that give rise to these salt-induced changes are not known. However, Bavykin et al. (1986) suggested on the basis of nuclease protection and DNA–histone cross-linking experiments that salt-induced compaction is accompanied by a migration of histone H1 from its location at the linker ee site to the linker proper. Such a rearrangement is consistent with our observations of subtle morphological changes at the linker ee sites in polynucleosomes at 40 mM NaCl, and merits further detailed study.

Returning to the question of why trinucleosomes should differ from higher oligomers in their response to salt, we note that although trinucleosomes incorporate a complete chromatosome, they may not contain a complete nucleosome-linker DNA unit. The center nucleosome has two linker DNA segments for VLR histone interaction, but the two outer nucleosomes do not, and this may lead to a different mode of VLR histone binding, especially if there is a significant interaction of the NH_2- and COOH-terminal domains with linker DNA. In this sense, the pentanucleosome is the smallest oligomer with one complete nucleosomal unit, and it is possible that a complete unit of this nature is required for the full salt response seen in higher polynucleosomes.

Recently, Hayes and Wolffe (1994) reconstituted histone octamers and the globular domain of histone H5 (GH5) onto a defined 168-bp sequence containing a strong nucleosome positioning sequence, and mapped the H5 contact sites. They concluded that GH5 was bound asymmetrically, and suggested that its primary effect was to bend DNA toward the histone octamer: the change in DNA path, rather than the direct effect of GH5 conferred the additional protection from micrococcal nuclease characteristic of the chromatosome. This model of the chromatosome suggests that the entering and exiting linker DNAs should leave tangentially from about the same location on the circumference of the nucleosome (Hayes and Wolffe, 1994), thus making an included angle of about 180°, rather than the ~60° observed in frozen hydrated preparations. Although the globular region of the VLR histones is sufficient to reconstitute the nuclease protection characteristic of the chromatosome, it requires the complete molecule to recover the zig-zag chromatin conformation (Allan et al., 1986). Until work on defined sequence reconstitutes is extended to include longer DNA segments and complete VLR histone molecules, it will not be possible to assess fully its implications for chromatin in general.

Compaction above 40 mM NaCl

Sedimentation data show that for the higher polynucleosomes (N = ~6+), there is a straight line relationship between log (S) and log (I) between 5.0 and 120 mM NaCl (Butler and Thomas, 1980; Bates et al., 1981), suggesting

that the compaction process is continuous over this salt range, without major changes in chromatin architecture. Conventional EM suggests that, at 40 mM NaCl, the low salt zig-zag morphology of isolated polynucleosomes has already condensed to the ultimate fiberlike conformation (Thoma et al., 1979; Woodcock et al., 1984). Although it will be important to extend our cryoelectron microscopy studies to higher salt concentrations, it is unlikely that this will reveal a major change in chromatin architecture, such as would be needed to convert a zig-zag structure to a helical solenoid. Preliminary studies of frozen hydrated polynucleosomes in 80 mM NaCl support this prediction.

Conclusions

The solution conformation of isolated polynucleosomes is seen by cryoelectron microscopy to be an irregular 3-D zig-zag, a conclusion also reached from an analysis of images obtained by scanning force microscopy (Zlatanova et al., 1994). This type of architecture appears to be consistent with physical measurements on isolated polynucleosomes (van Holde and Zlatanova, 1995). Irregular zig-zag structures are also generated from polynucleosome models in which nucleosome orientation is dictated by linker length (Woodcock et al., 1993; Leuba et al., 1994). Cryoelectron microscopy provides the means to test the basis of these models by examining the solution conformation of polynucleosomes reconstituted onto defined DNA sequences (Simpson et al., 1985).

Such observations are not limited to polynucleosomes in solution, or simulations thereof. A 3-D zig-zag has been observed in situ in tomographic reconstructions of chicken erythrocyte and starfish sperm nuclei (Horowitz et al., 1994). Further support for this type of architecture in situ has been obtained from observations of pyrimidine dimer formation in isolated nuclei (Pehrson, 1995).

As discussed in detail elsewhere (Woodcock and Horowitz, 1995), abandoning symmetry-based chromatin folding has several conceptual advantages. Difficulties with helical models, such as the reconciliation of solenoidal architectures with variable linker lengths (Felsenfeld and McGhee, 1984; Butler, 1984) disappear. More importantly, the plasticity of a dynamic, continuously variable 3-D zig-zag is fully consistent with the variety of structural and functional forms of chromatin.

We are grateful to Dr. David Hoagland, Department of Polymer Science and Engineering, University of Massachusetts, Amherst for making the dynamic light scattering apparatus available, and Dr. Noel Bonnet, University of Reims for providing source code for stereological analysis.

This work is supported by National Institutes of Health GM-43786 to C. L. Woodcock. The Microscopy and Imaging Facility, University of Massachusetts, Amherst, is supported in part by National Science Foundation BBS 87-14235.

Received for publication 18 July 1995 and in revised form 19 September 1995.

References

Adrian, M., J. Dubochet, J. Lepault, and A. W. McDowall. 1984. Cryo-electron microscopy of viruses. *Nature (Lond.).* 308:32–36.

Allan, J., P. G. Hartman, C. Crane-Robinson, and F. X. Aviles. 1980. The structure of histone H1 and its location in chromatin. *Nature (Lond.).* 288:675–679.

Allan, J., N. Harborne, D. C. Rau, and H. Gould. 1982. Participation of core histone "tails" in the stabilization of the chromatin solenoid. *J. Cell Biol.* 93: 285–297.

Allan, J., T. Mitchell, N. Harborne, P. Cattini, R. Craigie, and H. Gould. 1986. Roles of H1 domains in determining higher order chromatin structure and H1 location. *J. Mol. Biol.* 187:591–601.

Arents, G., R. W. Burlingame, B.-C. Wang, W. E. Love, and E. N. Moudrianakis. 1991. The nucleosomal core histone octamer at 3.1 A resolution: a tripartite protein assembly and a left-handed superhelix. *Proc. Natl. Acad. Sci. USA.* 88:10148–10152.

Bates, D. L., and J. O. Thomas. 1981. Histone H1 and H5: one or two molecules per nucleosome? *Nucleic Acids Res.* 9:5883–5894.

Bates, D. L., P. J. G. Butler, E. C. Pearson, and J. O. Thomas. 1981. Stability of the higher-order structure of chicken erythrocyte chromatin in solution. *Eur. J. Biochem.* 119:469–476.

Bavykin, S. G., S. I. Usachenko, A. O. Zalensky, and A. D. Mirzabekov. 1990. Structure of nucleosomes and organization of the internucleosomal DNA in chromatin. *J. Mol. Biol.* 212:495–511.

Bednar, J., P. Furrer, A. Stasiak, J. Dubochet, E. H. Egelman, and A. D. Bates. 1994. The twist, writhe and overall shape of supercoiled DNA change during counterion-induced transition from a loosely to a tightly wound superhelix. *J. Mol. Biol.* 235:825–847.

Bellare, J. R., H. T. Davis, L. E. Scriven, and Y. Talmon. 1988. Controlled environment vitrification system. An improved sample preparation technique. *Journal of Electron Microscopy Technique.* 10:87–111.

Beorchia, A., D. Ploton, M. Menager, M. Thiry, and N. Bonnet. 1991. Digital three-dimensional visualization of cellular organelles studied by medium- and high-voltage electron microscopy. *J. Microsc. (Oxf.).* 163:221–231.

Butler, P. J. G. 1984. A defined structure of the 30 nm fiber which accommodates different nucleosomal repeat lengths. *EMBO (Eur. Mol. Biol. Organ.) J.* 3:2599–2604.

Butler, P. J. G. 1988. The organization of the chromatin fiber. *In* Chromosomes and Chromatin. Vol 1. K. W. Adolph, editor. CRC Press, Boca Raton, FL. 57–82.

Butler, P. J. G., and J. O. Thomas. 1980. Changes in chromatin folding in solution. *J. Mol. Biol.* 140:505–529.

Caron, F., and J. O. Thomas. 1981. Exchange of histone H1 between different segments of chromatin. *J. Mol. Biol.* 146:513–537.

Clark, D. J., and T. Kimura. 1990. Electrostatic mechanism of chromatin folding. *J. Mol. Biol.* 211:883–896.

Cyrklaff, M., M. Adrian, and J. Dubochet. 1990. Evaporation during preparation of unsupported thin vitrified aqueous layers for cryo-electron microscopy. *Journal of Electron Microscopy Technique.* 16:351–355.

Dubochet, J., M. Adrian, J. J. Chang, J. C. Homo, J. Lepault, A. W. McDowall, and P. Schultz. 1988. Cryo-electron microscopy of vitrified specimens. *Q. Rev. Biophys.* 21:129–228.

Dubochet, J., M. Adrian, I. Dustin, P. Furrer, and A. Stasiak. 1992. Cryoelectron microscopy of DNA molecules in solution. *Methods Enzymol.* 211:507–518.

Dustin, I., P. Furrer, A. Stasiak, J. Dubochet, J. Langowski, and E. Egelman. 1991. Spatial visualization of DNA in solution. *J. Struct. Biol.* 107:15–21.

Felsenfeld, G. 1992. Chromatin as an essential part of the transcriptional mechanism. *Nature (Lond.).* 355:219–224.

Felsenfeld, G., and J. D. McGhee. 1986. Structure of the 30 nm chromatin fiber. *Cell.* 44:375–377.

Furrer, P., J. Bednar, J. Dubochet, A. Hamiche, and A. Prunell. 1995. DNA at the entry-exit of the nucleosome observed by cryoelectron microscopy. *J. Struct. Biol.* 114:177–183.

Garcia-Ramirez, M., F. Dong, and J. Ausio. 1992. Roll of the histone "tails" in the folding of oligonucleosomes depleted of histone H1. *J. Biol. Chem.* 267: 19587–19595.

Giannasca, P. J., R. A. Horowitz, and C. L. Woodcock. 1993. Transitions between in situ and isolated chromatin. *J. Cell Sci.* 105:551–561.

Hansen, J. C., J. Ausio, V. H. Stanik, and K. E. van Holde. 1989. Homogenous reconstituted oligonucleosomes. Evidence for folding in the absence of histone H1. *Biochemistry.* 28:9129–9136.

Hardison, R. C., D. P. Zeitler, J. M. Murphey, and R. Chalkley. 1977. Histone neighbors in nuclei and extended chromatin. *Cell.* 12:417–427.

Hayes, J. J., and A. P. Wolffe. 1993. Preferential and asymmetric interaction of linker histones with 5S DNA in the nucleosome. *Proc. Natl. Acad. Sci. USA.* 90:6415–6419.

Horowitz, R. A., P. J. Giannasca, and C. L. Woodcock. 1990. Ultrastructural preservation of nuclei and chromatin: improvements with low temperature methods. *J. Microsc. (Oxf.).* 157:205–224.

Horowitz, R. A., D. A. Agard, J. W. Sedat, and C. L. Woodcock. 1994. The three-dimensional architecture of chromatin in situ: electron tomography reveals fibers composed of a continuously variable zig-zag nucleosomal ribbon. *J. Cell Biol.* 125:1–10.

Lennard, A. C., and J. O. Thomas. 1985. The arrangement of H5 molecules in extended and condensed chicken erythrocyte chromatin. *EMBO (Eur. Mol. Biol. Organ.) J.* 4:3455–3462.

Leuba, S. H., G. Yang, C. Robert, B. Samori, K. van Holde, J. Zlatanova, and C. Bustamente. 1994. Three-dimensional structure of extended chromatin fibers as revealed by tapping-mode scanning force microscopy. *Proc. Natl. Acad. Sci. USA.* 91:11621–11625.

Losa, R., F. Thoma, and T. Koller. 1984. Involvement of the globular domain of histone H1 in the higher order structure of chromatin. *J. Mol. Biol.* 175:529–551.

Marion, C., P. Bezot, C. Hesse-Bezot, B. Roux, and J.-C. Bernengo. 1981. Conformation of chromatin oligomers. A new argument for a change with the hexanucleosome. *Eur. J. Biochem.* 120:169–176.

Pehrson, J. R. 1995. Probing the conformation of nucleosome linker DNA in situ with pyrimidine dimer formation. *J. Biol.Chem.* 270:1–5.

Pennings, S., G. Meersseman, and E. M. Bradbury. 1991. Mobility of positioned nucleosomes on 5S rDNA. *J. Mol. Biol.* 220:101–110.

Pennings, S., G. Meersseman, and E. M. Bradbury. 1994. Linker histones H1 and H5 prevent the mobility of positioned nucleosomes. *Proc. Natl. Acad. Sci. USA.* 91:10275–10279.

Provencher, S. W. 1982. CONTIN: a general purpose constrained regularization program for inverting noisy linear algebraic and integral equations. *Computational Physics Communications.* 27:229–242.

Prunell, A., and R. D. Kornberg. 1982. Variable center to center distance of nucleosomes in chromatin. *J. Mol. Biol.* 154:515–523.

Rattner, J. B., and B. A. Hanikalo. 1978. Higher order structure in metaphase chromosomes. *Chromosoma (Berl.).* 69:363–379.

Richmond, T. J., J. T. Finch, B. Rushton, D. Rhodes, amd A. Klug. 1984. The structure of the nucleosome core particle at 7A resolution. *Nature (Lond.).* 311:532–537.

Simpson, R. T. 1978. Structure of the chromatosome, a chromatin particle containing 160 base pairs of DNA and all the histones. *Biochemistry.* 17:5524–5531.

Simpson, R. T., F. Thoma, and J. M. Brubaker. 1985. Chromatin reconstituted from tandemly repeated cloned DNA fragments and core histones: a model system for study of higher order structure. *Cell.* 42:799–808.

Stuart, M., and G. Vigers. 1986. Electron microscopy of frozen-hydrated biological material. *Nature (Lond.).* 319:631–636.

Thoma, F., and T. Koller. 1977. Influence of histone H1 on chromatin structure. *Cell.* 12:101–107.

Thoma, F., and T. Koller. 1981. Unravelled nucleosomes, nucleosome beads, and higher order structures of chromatin: influence of non-histone components and histone H1. *J. Mol. Biol.* 14:709–733.

Thoma, F., T. Koller, and A. Klug. 1979. Involvement of histone H1 in the organization of the nucleosome and the salt-dependent superstructures of chromatin. *J. Cell Biol.* 83:403–427.

Thomas, J. O., and C. Rees. 1983. Exchange of histones H1 and H5 between chromatin fragments: a preference of H5 for higher-order structures. *Eur. J. Biochem.* 134:109–115.

Todd, R. D., and W. T. Garrard. 1979. Overall pathway of mononucleosome production. *J. Biol. Chem.* 254:3074–3083.

van Holde, K. E. 1988. Chromatin. Springer-Verlag New York Inc., New York. 497 pp.

van Holde, K. 1993. The omnipotent nucleosome. *Nature (Lond.).* 362:111–112.

van Holde, K., and J. Zlatanova. 1995. Chromatin higher order structure: chasing a mirage? *J. Biol. Chem.* 270:8373–8376.

Vigers, G. P. A., R. A. Crowther, and B. M. F. Pearse. 1986. Three-dimensional structure of clathrin cages in ice. *EMBO (Eur. Mol. Biol. Organ.) J.* 3:529–534.

Wade, R. H., and D. Chretien. 1993. Cryoelectron microscopy of microtubules. *J. Struct. Biol.* 110:1–27.

Widom, J. 1986. Physiochemical studies of the folding of the 100A nucleosome filament into the 300A filament. cation dependence. *J. Mol. Biol.* 190:411–424.

Widom, J. 1989. Toward a unified model of chromatin folding. *Annu. Rev. Biophys. Biophys. Chem.* 18:365–395.

Williams, S. P., and J. P. Langmore. 1991. Small angle x-ray scattering of chromatin. Radius and mass per unit length depend on linker length. *Biophys. J.* 59:606–618.

Wolffe, A. P. 1994. Transcription: in tune with the histones. *Cell.* 77:13–16.

Woodcock, C. L. 1994. Chromatin fibers observed in situ in frozen hydrated sections. Native fiber diameter is not correlated with nuclessome repeat length. *J. Cell Biol.* 125:11–19.

Woodcock, C. L., L.-L. Y. Frado, G. R. Green, and L. Einck. 1981. Adhesion of particulate specimens to support films for electron microscopy. *J. Microsc. (Oxf.).* 121:211–220.

Woodcock, C. L., L.-L. Y. Frado, and J. D. Rattner. 1984. The higher-order structure of chromatin: evidence for a helical ribbon arrangement. *J. Cell Biol.* 99:42–52.

Woodcock, C. L., S. A. Grigoryev, R. A. Horowitz, and N. Whitaker. 1993. A chromatin folding model that incorporates linker variability generates fibers resembling the native structures. *Proc. Natl. Acad. Sci. USA.* 90:9021–9025.

Woodcock, C. L., and R. A. Horowitz. 1995. Chromatin organisation re-viewed. *Trends Cell Biol.* 5:272–277.

Yao, J., P. T. Lowary, and J. Widom. 1990. Direct detection of linker DNA bending in defined-length oligomers of chromatin. *Proc. Natl. Acad. Sci. USA.* 87:7603–7607.

Yao, J., P. T. Lowary, and J. Widom. 1991. Linker DNA bending induced by the core histones of chromatin. *Biochemistry.* 30:8408–8414.

Yao, J., P. T. Lowary, and J. Widom. 1993. Twist constraints on linker DNA in the 30-nm chromatin fiber: implications for nucleosome phasing. *Proc. Natl. Acad. Sci. USA.* 90:9364–9368.

Zivanovic, Y., I. Duband-Goulet, P. Schultz, E. Stofer, P. Oudet, and A. Prunell. 1990. Chromatin reconstitution on small DNA rings III. Histone H5 dependence of DNA supercoiling in the nucleosome. *J. Mol. Biol.* 214:479–485.

Zlatanova, J., S. H. Leuba, G. Yang, C. Bustamente, and K. van Holde. 1994. Linker DNA accessibility in chromatin fibers of different conformations: a reevaluation. *Proc. Natl. Acad. Sci. USA.* 91:5277-5280.